Coordination Chemistry Reviews
206–207 (2000) 285–319

COORDINATION
CHEMISTRY
REVIEWS

www.elsevier.com/locate/ccr

# Low valent aluminum and gallium compounds — structural variety and coordination modes to transition metal fragments

G. Linti [1], H. Schnöckel *

*Institut für Anorganische Chemie der Universität Karlsruhe (TH), Engesserstrasse, Geb. 30.45,
76128 Karlsruhe, Germany*

Received 27 September 1999; received in revised form 7 February 2000; accepted 7 February 2000

**Contents**

---

* Corresponding author. Tel.: + 49-721-6082981; fax: + 49-721-6084854.

*E-mail addresses:* linti@aklinti.oci.uni-heidelberg.de (G. Linti), hg@achpc9.chemie.uni-karlsruhe.de (H. Schnöckel).

[1] Present address: Anorganisch-Chemisches Institut der Universität Heidelberg, Im Neunheimer Feld 270, 69120 Heidelberg, Germany.

PII: S0010-8545(00)00339-8

## Abstract

The chemistry of low valent aluminum and gallium compounds is a very topical area of research. Accompanying the preparative challenge in synthesizing novel types of main group cluster compounds and transition metal complexes with aluminum and gallium ligands, an area of chemistry is being exploited, which requires new insight on the description of chemical bonds. Therefore, not only are routes to these compounds and their structures described here, but thoughts on the description of bonding are presented as well.

*Keywords:* Aluminum; Gallium; Transition metals; Clusters; Low valent

---

## 1. Introduction

As evidenced by even the most recent inorganic textbooks, the + III oxidation state is still being taught as the dominant, if not the only, oxidation state of aluminum and gallium. It was only in the last decade of the past millennium, that the chemistry of low valent compounds of the heavier Group 13 elements made rapid progress. Driven by the fascination of metal–metal bonded species a series of new cluster compounds of these elements has been synthesized and characterized. In the meantime a structural variety has been reached, which has in many cases no analogies by other elements. Not even the well-explored chemistry of the lightest element in this group — boron — which is well understood, can compete with it.

The study of these compounds with Group 13–Group 13 element bonds fertilized investigations on the coordination behavior of monovalent Group 13 derivatives to transition metal fragments. The following scope will mainly be confined to aluminum and gallium compounds with cyclopentadienyl and tris(trimethylsilyl)silyl (hypersilyl) ligands, which are preferentially used in this kind of chemistry.

## 2. Routes to low valent aluminum and gallium compounds

In principle, two different routes to synthesize low valent aluminum and gallium compounds are applied: The dehalogenation of $R_2EX$ and $REX_2$ ($E = Al$, Ga; $X =$ halide) (Section 2.1) and the substitution of halide in subhalides (Section 2.2).

### 2.1. Dehalogenation of $R_2EX$ and $REX_2$

The straightforward method to prepare low valent aluminum and gallium compounds is the dehalogenation of $R_2EX$ and $REX_2$ species (Scheme 1). That means, starting from compounds with aluminum and gallium in oxidation state + III reducing agents like alkali metals, Riecke magnesium as well as $NaSi^tBu_3$ are used (Eq. (1a) and (b)).

$$R_2EX + 2M \rightarrow 2MX + R_2E\text{–}ER_2 \quad E = Al, Ga; \quad X = \text{halide};$$
$$M = \text{alkalimetal} \tag{1a}$$

$$REX_2 + 4M \rightarrow 4MX + (RE)_n \quad n = 1, \ldots, 4 \tag{1b}$$

$$EX + MR \rightarrow MX + (RE)_n \tag{1c}$$

This method has been applied by various groups to achieve organometallic substituted dialanes and digallanes $R_4E_2$ (**1**), the chemistry of which has been extensively reviewed [1], while tetrahedral compounds $E_4R_4$ (**2**) will be discussed below. By reductions of compounds of type **1** also ionic and radical species have been obtained, namely icosahedral **3** [2] the anionic gallanes **4** [3] and **5** [4] and the digallanyl **6** [5]. Complex **4**, has been especially discussed [6], because the authors controversially claimed the existence of a gallium–gallium 'triple' bond, an assumption, which was more or less supported by a few theoreticians [7].

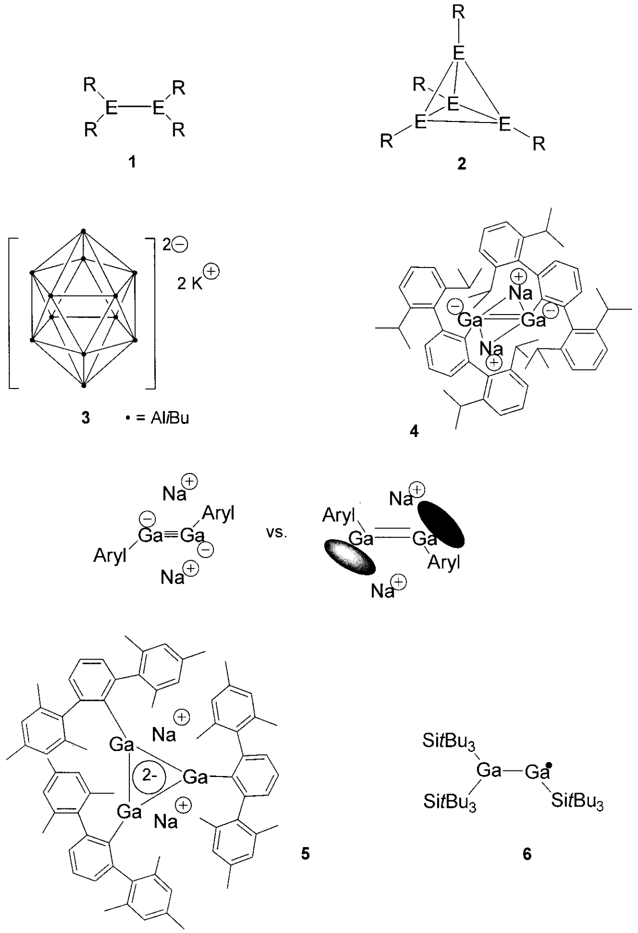

Scheme 1.

Table 1
Calculated [9] force constants $f$ (mdyn Å$^{-1}$) and distances $d$ (pm) of species containing 'triple', 'double', and 'single' Ga–Ga as well as the corresponding As–As bonds (exp. data in brackets [11]).

| | $Ga_2H_6^{2-}$ ($D_{3d}$) Ga–Ga | $Ga_2H_4^{2-}$ ($C_{2h}$) Ga=Ga bonding | $Ga_2H_2^{2-}$ ($C_{2h}$) Ga≡Ga |
|---|---|---|---|
| $f$(Ga–Ga) | 0.75 | 0.98 | 1.01[a] |
| $d$(Ga–Ga) | 257.8 | 245.6 | 241.0 |
| | $As_2H_4$ As–As | $As_2H_2$ As=As bonding | $As_2$ As≡As |
| $f$(As–As) | 1.56 | 2.61 | 4.22 (4.08) |
| $d$(As–As) | 249 | 227 | 212 (210) |

[a] For $Na_2[Ga_2H_2]$ with $Na^+$ ions above and below the Ga–Ga bond ($C_{2h}$ symmetry): $f$(Ga–Ga) = 1.03.

The short Ga–Ga distance in **4** (232 pm) [3] could almost be confirmed by quantum chemical calculations if large ligands are involved containing aryl rings for sandwiching the $Na^+$ cations [6b]. However, these calculations show that there is only a marginal difference between Ga–Ga 'triple' and 'double' bonding concerning the bond lengths and that the potential energy curves are flat in both cases. Continuing these considerations, we want to introduce a further aspect into this discussion, which is based on force constants [8].

In order to get a confidential Ga–Ga force constant the vibrational spectrum, especially the Raman spectrum, is necessary. Since there is almost no chance of obtaining this complete set of experimental values, they should be extracted from quantum chemical calculations [9], which seems to be reasonable because, to date, computational methods have been developed to such a high standard that calculated frequencies are mostly in good agreement with experimental results. We carried out these procedures for the dianions $Ga_2H_2^{2-}$, $Ga_2H_4^{2-}$, and $Ga_2H_6^{2-}$ and performed a transformation of the force constants (Cartesian coordinates) to those of the GVFF (general valence force field) [10]. The results, i.e. the Ga–Ga force constants and distances are summarized in Table 1.

It is important to note that the Ga–Ga distances show the expected trend, however, the Ga–Ga force constants exhibit a very weak bond, which shows only a slight increase going from $Ga_2H_4^{2-}$ to $Ga_2H_2^{2-}$ (c.f. Table 1). To bring the problems on the point, with respect to the Ga–Ga force constants no hints for any Ga–Ga multiple bonding can be detected. This unexpected result will be more impressive and convincing if it is compared with the calculated results for the isoelectronic species $As_2$, $As_2H_2$, and $As_2H_4$, which are also presented in Table 1. For these molecules force constants, distances, theory, and chemical intuition are in line with triple, double and single bonding. The reason for the discrepancy between the $As_2$ and the $Ga_2$ species shall not be discussed here, but the consequences are described below.

If the nomenclature of multiple bonding shall have any meaning — in the normal language bonding means that two things are bonded together and multiple means an approximately $n$-times stronger bonding — then one should not speak about Ga–Ga multiple bonds concerning the species under discussion! However, we have to decide, whether a bond may be regarded as a bond only on the basis of the occupation of certain MOs or on chemical bonding forces, which in principle can be obtained experimentally. A further measure of bond strength is the dissociation energy, which is not as suitable as force constants are for this purpose, since bonding (geometric and electronic) within the fragments ($GaH^-$, $GaH_2^-$, $GaH_3^-$ in an infinite separation) is different from the bonding situation in the dimeric species (e.g. $Ga_2H_2^{2-}$). In contrast, force constants are a much more suitable measure, since only infinitely small changes in the bond distances are necessary to detect the restoring forces [10c]. To sum up, since we prefer experimental findings to give a necessary basis for important statements in chemistry, we would consider the Ga–Ga bonds under discussion to be weak in any case. Obviously this bond is not strengthened when additional electrons occupy the π-MOs, since these MOs are non-bonding. That is, by occupation of non-bonding MOs no multiple bonds can be generated. However, for the isoelectronic $As_2$ species (Table 1) the situation is completely different, since experimental as well as theoretical findings are in line with chemical intuition. Therefore, in this case no problem exists in the nomenclature, however, if there are discrepancies as in the '$Ga_2$' case we would suggest a nomenclature that is more adopted to the experiment than to the theoretical findings until the whole story is understood [6].

## 2.2. Substitution of subhalides

The second, more sophisticated method to obtain low valent aluminum and gallium compounds involves salt elimination from subhalides of these elements (Eq. (1c)). However, only a few gallium subhalides can be prepared conventionally by comproportionation ($2Ga + 4GaX_3 \rightarrow 3Ga_2X_4$). It was only in the early 1980s, that some dihalides of the type two donor $Ga_2X_4$ (X = Cl, Br, I; donor = dioxane, pyridine, phosphanes, X) [12] with preformed gallium–gallium bonds was characterized. Also about 10 years ago for GaI a simple synthesis was described [13]. Here, gallium and iodine are activated in toluene by ultrasound. The greenish, temperature stable powder obtained — which by the way has not been structurally characterized so far — undergoes reactions, which are indicative for a potential gallium(I) halide (Eq. (2)). In the presence of GaI (Eq. (2)) disproportionation is observed to afford the gallium iodides $Ga_2I_4 \cdot 2PEt_3$ (**7**) (Fig. 1) and $Ga_3I_5 \cdot 3PEt_3$ (**8**) (Fig. 2) [14]. Remarkable is the generation of gallium(I) pyrazolylborate (**9**) [15].

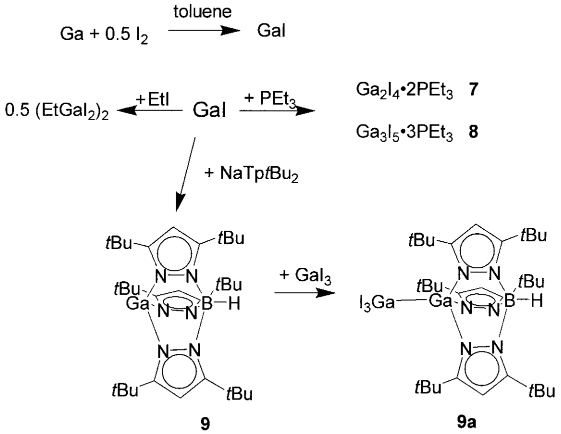

(2)

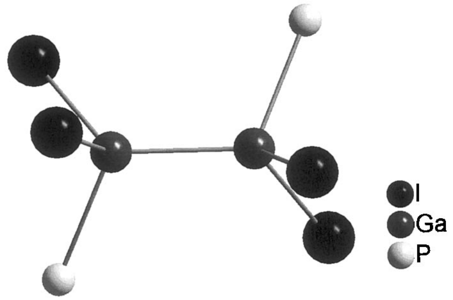

Fig. 1. View of a molecule of **7**.

Only recently have aluminum analogs $Al_2X_4 \cdot 2$ donor compounds been reported [16]. These are by-products in the disproportionation process of solutions containing aluminum(I) halides. The general way to obtain such metastable EX solutions (E = Al, Ga; X = Cl, Br, I) is by trapping the high-temperature monohalides EX [17]. This method was described first for AlCl [18] and later on it was applied for all other EX species. The principle of this technique is simple, but for technical realization some experience is necessary. At ca. 1000°C and low pressure ($10^{-2}$ mbar) EX molecules are stable with respect to formation of $EX_3$ and E (e.g. $2Al(l) + AlCl_3(g) \rightarrow 3AlCl(g)$). Thus, by passing gaseous HX over heated aluminum under the above mentioned conditions nearly pure AlX is formed. Condensation of the high-temperature gas at −196°C together with toluene–donor solvent mixtures affords solutions which are metastable (with respect to disproportionation) up to ambient temperatures, depending on the halide and donor used. Besides products of disproportionation like $Ga[GaCl_2(OEt_2)]_3[GaCl(OEt_2)_2]$ [19] from these solutions the first crystalline aluminum and gallium monohalides could be isolated as tetrameric $Al_4X_4 \cdot 4$ donor (**10**) [20] (Fig. 3) and octameric species $Ga_8I_8 \cdot 6PEt_3$ (**11**) (Fig. 4) [21]. With thf as a donor the first polyhedral aluminum subhalide (**12**) was obtained (Fig. 5) [22]. Here a central $Al_{12}$ icosahedron bears ten $AlBr_2(thf)$

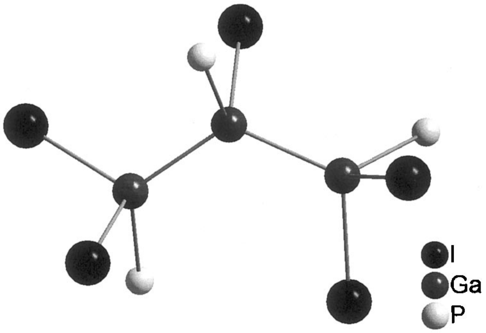

Fig. 2. View of a molecule of **8**.

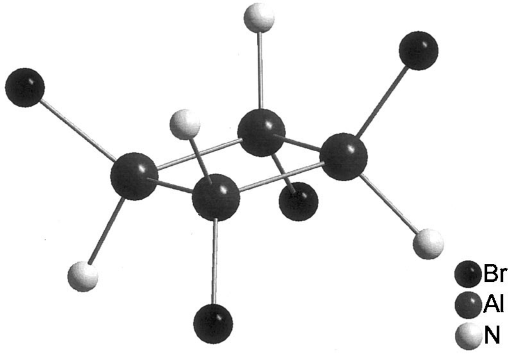

Fig. 3. View of a molecule of **10**.

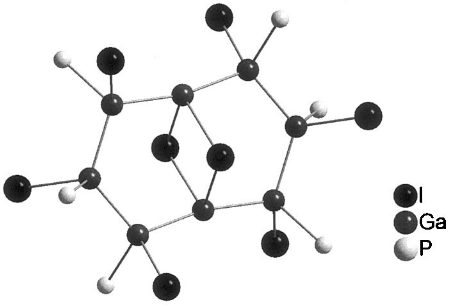

Fig. 4. View of a molecule of **11**.

substituents and two thf molecules at the apical aluminum atoms. According to the Wade–Rudolph rules **12** is a *closo* polyhedron with 13 cluster-binding electron pairs. Obviously, an internal disproportionation has proceeded in the AlBr solu-

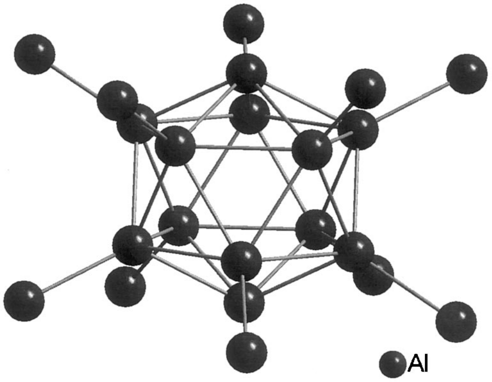

Fig. 5. View of a molecule of **12**.

tion: an $Al_{12}$ core ($Al^0$) connected to ten $AlX_2$ units ($Al^{+II}$) is formed. From DFT calculations it has been concluded, that the bottom of the thermodynamical ladder — $Al_{solid} + AlBr_3$ — is nearly reached by formation of **12**, which is regarded as a possible intermediate on the way to a new modification of aluminum.

## 3. Organyl and silyl derivatives of aluminum and gallium in oxidation state +I

In 1991 — nearly simultaneously with the icosahedral $Al_{12}$ dianion $[Al_{12}({}^iBu)_{12}]^{2-}$ (**3**) — the first neutral polyhedral aluminum compound $(cp^*Al)_4$ (**13**) was prepared starting from metastable aluminum(I) halides solutions (Eq. (3a)) [23]. An alternative synthesis (Eq. (3b)) was later developed [24]. Cp* gallium(I) **14** and other gallium cp derivatives were synthesized analogously (Eq. (4)), originally from gallium(I) halides [17,25a,26] and afterwards in a facile high-yield synthesis via reduction of $[cp^*GaI_2]$ [27].

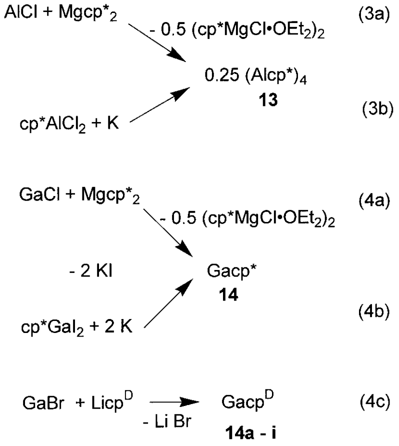

Other cyclopentadienyl derivatives ($cp^D$) of aluminum [28] and gallium [25a] are accessible in analogy to (Eqs. (3) and (4)). These are summarized in Table 2.

In the solid state **13** exhibits a tetrahedral $Al_4$ core with Al–Al distances of 276.9 pm (Fig. 6). In contrast, Gacp* (**14**) forms hexameric aggregates in the solid state [29] (Fig. 7) and is thus isomorphous to $(cp^*In)_6$ [30]. Due to long gallium–gallium distances ($d_{Ga-Ga} = 407.3–417.3$ pm) in this distorted octahedral arrangement, which are even longer than the In–In contacts in $(cp^*In)_6$, it was proposed that both clusters are held together by van der Waals interactions between the cp* ligands and not the metal–metal bonds. In contrast, **13** as a cluster with four cluster-binding electron pairs is held together by four 2e3c bonds on the four facets of the tetrahedron. Contrary to their various aggregation modes in the solid state, all Mcp* derivatives (M = Al, Ga, In, Tl [31]) vaporize as monomeric molecules. The gas phase structure of **14** determined by electron scattering is depicted in Fig. 8 [32]. Efforts have been taken to use the volatility of these compounds for MOCVD procedures, but **14** proved to be thermally stable up to 600°C [27].

Table 2
Cyclopentadienyl derivatives of aluminum(I) and gallium(I)

| Compound | | Aggregation in solution 4 $cp^DE/(cp^DE)_4$ | Synthesis | Literature |
|---|---|---|---|---|
| cp*Al | **13** | Monomer/tetramer[a] | Eqs. (3) and (5c) | [17,23,24,28] |
| cpAl | **13a** | Tetramer[a] | Eq. (3a) | [17] |
| $C_5Benzyl_5Al$ | **13b** | Monomer[a] | Eq. (5b) | [28] |
| $C_5H_2(SiMe_3)_3Al$ | **13c** | Monomer[a] | Eq. (5c) | [28] |
| $C_5H_4^tBuAl$ | **13d** | Tetramer[a] | Eq. (5c) | [28] |
| $C_5H(^iPr)_4Al$ | **13e** | Monomer[a] | Eq. (5c) | [28] |
| $C_5H_3(SiMe_3)_2Al$ | **13f** | Monomer/tetramer[a] | Eq. (5c) | [28] |
| $(cp^*Al)_3Alcp$ | **15** | Tetramer[a] | Eq. (5a) | [28] |
| $(cp^*Al)_3AlN(SiMe_3)_2$ | **16** | Tetramer[a] | Eq. (5a) | [28] |
| cp*Ga | **14** | (Monomer) | Eq. (4) | [25a] |
| cpGa | **14a** | (Monomer) | Eq. (4a) | [26] |
| $(C_4P)H_2(^tBu)_2Ga$ | **14b** | (Monomer) | Eq. (4c) | [64] |
| $C_5H_4^tBuGa$ | **14c** | (Monomer) | Eq. (4c) | [25a] |
| $C_5H_4(^iPr)Ga$ | **14d** | (Monomer) | Eq. (4c) | [25b] |
| $C_5H(^iPr)_4Ga$ | **14e** | (Monomer) | Eq. (4c) | [25c] |
| $C_5Benzyl_5Ga$ | **14f** | (Monomer) | Eq. (4c) | [25a] |
| $C_5H_2(SiMe_3)_3Ga$ | **14g** | (Monomer) | Eq. (4c) | [25a] |
| $C_5Me_4EtGa$ | **14h** | (Monomer) | Eq. (4c) | [25c] |
| $C_5Ph_5Ga$ | **14i** | (Monomer) | Eq. (4c) | [25c] |

[a] By means of $^{27}Al$-NMR spectroscopy [28].

Compounds like **13** and **14** are valuable starting materials for new organo aluminum and gallium compounds. Thus mixed tetrahedral aluminum clusters $(cp^*Al)_3AlR$ (**15**) and (**16**) are available from **13** and LiR (Eq. (5)) [28]. Complex **16**, which was the first structurally characterized aluminum(I) amide (Fig. 9) is especially mentioned. The introduction of an $AlN(SiMe_3)_2$ group into the $Al_4$ cluster affords — compared to **13** — a considerable shortening of those Al–Al distances,

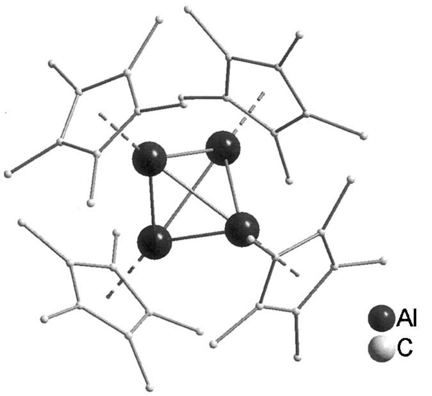

Fig. 6. View of a molecule of **13**.

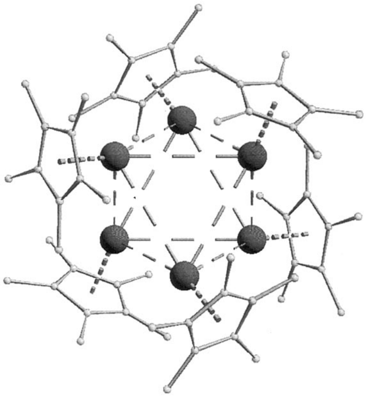

Fig. 7. View of a molecule of **14**.

in which the Al–N group is involved: d($Al_{cp*}$–$Al_N$) = 263.2–268.6 pm and d($Al_{cp*}$–$Al_{cp*}$) = 275.6–276.3 pm. According to quantum chemical calculations the cluster bonding of tetrahedral $Al_4$ cores is substantially influenced by the different electronic properties of the ligands (π back-bonding, induction effect) that is evidenced experimentally by this and the following examples of tetrahedral $Al_4$ compounds [28].

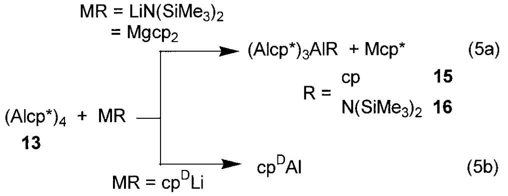

$$(\mathrm{Alcp^*})_4 + \mathrm{MR} \xrightarrow{\mathrm{MR = LiN(SiMe_3)_2\ = Mgcp_2}} (\mathrm{Alcp^*})_3\mathrm{AlR} + \mathrm{Mcp^*} \qquad \mathrm{R} = \mathrm{cp}\ \mathbf{15},\ \mathrm{N(SiMe_3)_2}\ \mathbf{16} \tag{5a}$$

$$\underset{\mathbf{13}}{(\mathrm{Alcp^*})_4} + \mathrm{MR} \xrightarrow[\mathrm{MR = cp^DLi}]{} \mathrm{cp^DAl} \tag{5b}$$

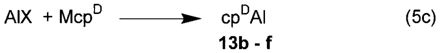

$$\mathrm{AlX} + \mathrm{Mcp^D} \longrightarrow \underset{\mathbf{13b - f}}{\mathrm{cp^DAl}} \tag{5c}$$

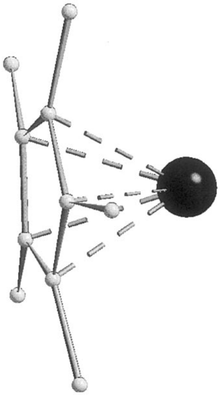

Fig. 8. Gas phase structure of a molecule of **14**.

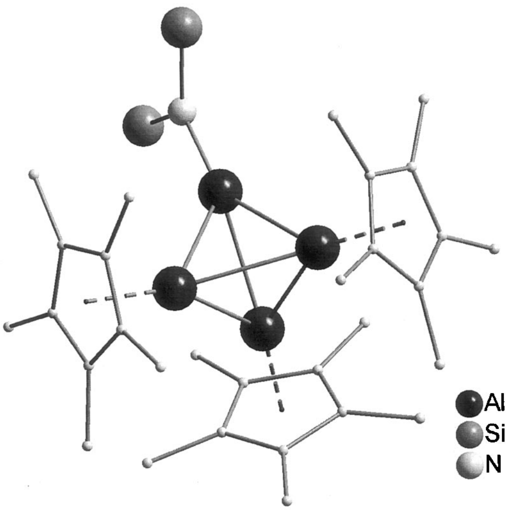

Fig. 9. View of a molecule of **16**.

The hypersilyl ligand stabilizes the tetrahedral aluminum and gallium compounds **17** and **18** via short Al–Al and Ga–Ga bonds. Complex **17** is synthesized by a metathesis reaction between tetrameric aluminum(I) bromide and Li(thf)$_3$Si(SiMe$_3$)$_3$ (Eq. (6)) [33]. Similarly, [Al(Si$^t$Bu)$_3$]$_4$ (**19**) is obtained from tetrameric aluminum(I) iodide **7** and NaSi$^t$Bu$_3$ [34]. Another alumatetrahedrane, [AlC(SiMe$_3$)$_3$]$_4$ (**20**) was prepared according to Eq. (1b) [35]. For the preparation of the corresponding gallium compounds various methods have been applied. Originally, **21a** [36] and **18** [37] were prepared by reaction of Ga$_2$X$_4$ · 2 dioxane and the lithiated ligands in pentane (Eq. (7)). Hence, a disproportionation reaction of the gallium(II) halides is implied here and thus only minor yields of the tetrahedranes are available. **21a** and other C(SiR$_2$R′)$_3$ substituted derivatives **21b** are obtained in good yields by reduction of the appropriate tri-iodogallates with magnesium according to (Eq. (1b)) [38]. The Si$^t$Bu$_3$ substituted gallatetrahedrane **22** is synthesized by thermolysis of **6** (Eq. (8)) [39].

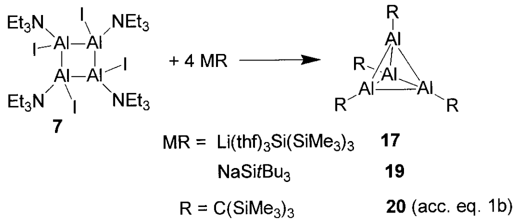

(6)

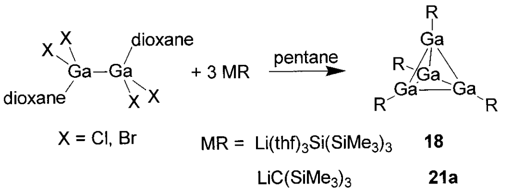

(7)

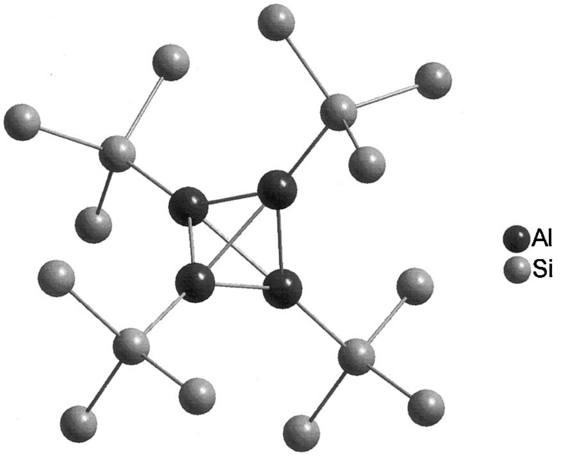

Fig. 10. View of a molecule of **17**.

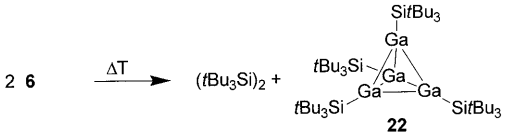

(8)

Comparing the silyl substituted tetrahedranes **17** (Fig. 10), **18** (Fig. 11), **19**, and **22** with the organyl substituted ones, **13**, **20**, and **21**, considerably shorter Al–Al and Ga–Ga distances are observed (Table 3). This is in line with the dissociation behavior of these compounds. **13**, **20**, and **21** monomerize in solution and in their mass spectra only fragmentation to $(ER)^{\bullet+}$ is observed. The structure of the

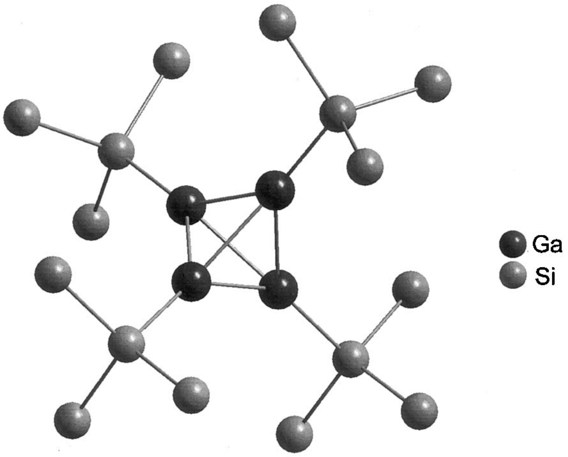

Fig. 11. View of a molecule of **18**.

Table 3
Experimentally determined and calculated properties of organyl and silyl substituted tetrahedranes $R_4E_4$

| Compound | $d_{\mathrm{E-E}}^{\mathrm{exp}}$ (pm) | $\lambda_{\mathrm{max}}$ (nm) | $d_{\mathrm{E-E}}^{\mathrm{DFT}}$ (pm) | $E_{\mathrm{tetra}}$ (kJ mol$^{-1}$) |
|---|---|---|---|---|
| **13** | 277.0 [23] | 372 | – | −160 [17] |
| **20** | 274.0 [35] | 418 | – | – |
| **17** | 260.2 [33] | 540 | – | – |
| **19** | 260.4 [34] | – | 265.5 | −606 [34] |
| **21a** | 268.8 [36] | 435 | 273.8 | −197[a] |
| **18** | 258.8 [37] | 554 | 261.6 | −419[a] |
| **22** | 257.9 [39] | – | 260.7 | −499[a] |

[a] See Ref. [52].

monomer of **21a** $(Me_3Si)_3CGa$ could be determined by electron scattering in the gas phase [40]. In contrast, in the mass spectra of the silyl substituted tetrahedranes the molpeaks $(ER)_4^{\bullet +}$ occur in high intensities. This behavior gives strong experimental evidence for stronger metal–metal interactions in these compounds.

## 4. Subvalent compounds

### 4.1. Aluminum

Since **13** can be obtained on a gram scale via different routes (Eqs. 3(a) and (b)) it might be a powerful reagent in many fields of chemistry in the future, e.g. in organic synthesis, and it is a suitable precursor for further subvalent species. The reaction with $(As^tBu)_4$ (Eq. (9)) ends up with $As_2(Alcp^*)_3$ **23** [41], a molecule with a *closo* type $As_2Al_3$ core (Fig. 12). Reaction of **13** with $Al_2I_6$ (Eq. (10)) allows the

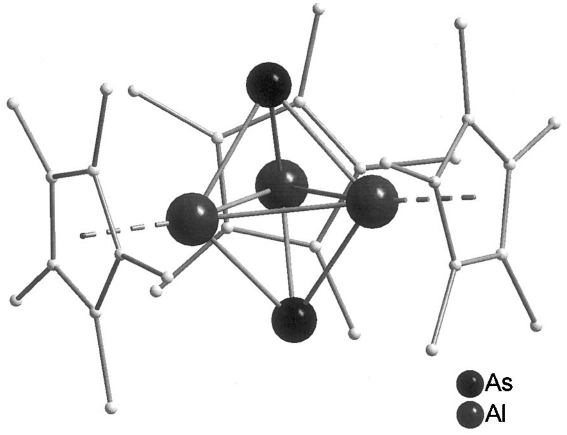

Fig. 12. View of a molecule of **23**.

isolation of **2** (Fig. 13) via insertion reactions of Alcp* fragments into Al–I bonds [42]. The formation of **24** leads to the conclusion, that aluminum(I) compounds may be essential intermediates during the electrochemical reduction of organo aluminum compounds.

Hence, remarkable sources in the cluster chemistry of aluminum have its origin in metastable AlX solutions. Besides the formation of tetrahedral species, discussed above, only a single example for an octahedral $Al_6$ cluster could so far be obtained by this method: $[Al_6(^tBu)_6]^{\bullet-}$ (**25**) (Eq. (11)) [43]. Structure and bonding of this unique ion have been elucidated by ESR spectroscopy supported by quantum chemistry.

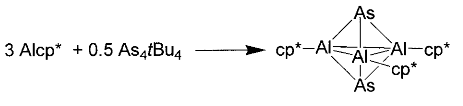

**23**

(9)

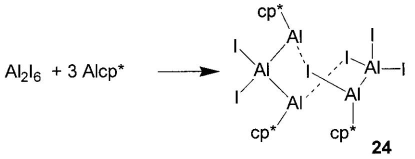

(10)

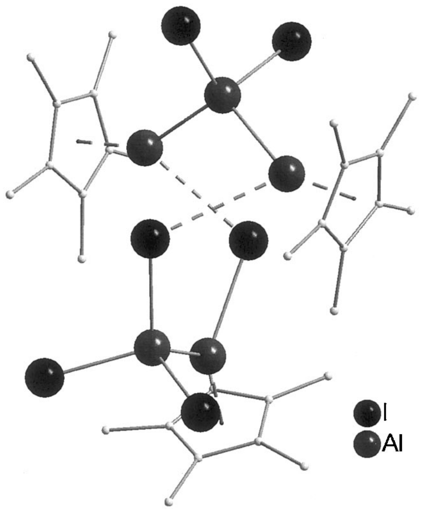

Fig. 13. View of a molecule of **24**.

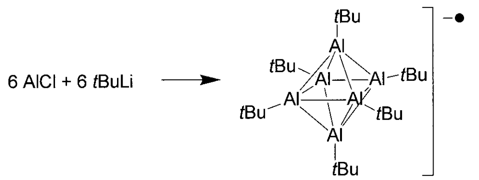

**25**

(11)

However, the most interesting results achieved via substitution of the halide atoms by bulky ligands, point into an entirely novel field of cluster chemistry. While disproportionation of AlX solutions towards metal and $AlX_3$ proceeds between −20 and 50°C — depending on the donor applied — intermediates on the way to metal formation can be trapped in the presence of bulky ligands. This mild method makes metal-rich clusters available, in which the ratio of the number of metal–metal bonds to metal–ligand bonds is growing the more the bulk metal is approached. For these novel kinds of metal clusters we suggest the nomenclature 'metalloidal clusters' [44], because the number of real, unbridged metal–metal bonds is larger than that of the 2e2c metal–ligand bonds. These novel clusters could be structurally characterized and, therefore, they allow for the first time an insight into the formation of solid metals, which is one of the oldest chemical processes known to mankind. On the other hand, such metalloidal clusters may be intermediates during the dissolution of metals.

The most remarkable step in this field was the formation of an $Al_{77}R_{20}$ cluster [$R = N(SiMe_3)_2$] (**26**) from AlI solutions and LiR (Eq. (12)) [45]. This is indeed a metalloidal cluster, since the 20 AlR bonds have to be compared with the many Al–Al contacts within the $Al_{57}$ core (Fig. 14). This species is by far the largest metalloidal cluster, which has been structurally characterized. Although, a great number of large gold and palladium clusters are known, most of them have, so far, not been crystallized [46]. Therefore, they are described on geometrical arguments as small pieces of metal surrounded by a ligand shell to prevent the formation of bulk metal. However, the structural characterization of the $Al_{77}$ cluster results in a quite different, but very plausible picture. From the center to the outer shell the coordination number of the aluminum atoms decreases from 12 to four, and simultaneously the Al–Al distances shrink. That is, the bonding character of the aluminum atoms may be described as metalloid in the center and as molecular in the $(AlR)_{20}$ shell. As far as we know, this picture of a metalloidal cluster based on an experimentally determined structure is new. Neither modern methods of electron microscopy nor quantum chemical calculations have been able to solve this problem, i.e. providing a proper description based on experimental results for the structural transition between a molecular compound and bulk metal. Obviously, experimental chemistry combined again with X-ray structure determination was the essential step into a new area of chemistry.

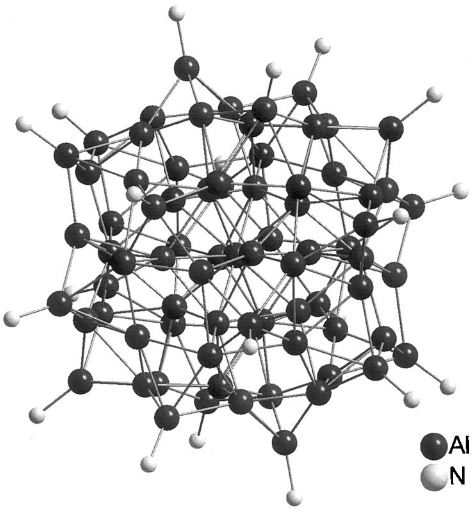

Fig. 14. View of the anion $Al_{77}[N(SiMe_3)_2]_{20}^{2-}$ **26**.

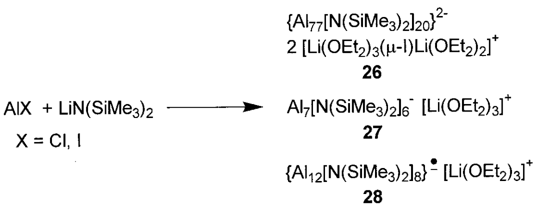

$$\begin{array}{lcl} & & \{Al_{77}[N(SiMe_3)_2]_{20}\}^{2-} \\ & & 2\,[Li(OEt_2)_3(\mu\text{-}I)Li(OEt_2)_2]^+ \\ & & \mathbf{26} \\ AlX + LiN(SiMe_3)_2 & \longrightarrow & Al_7[N(SiMe_3)_2]_6^- \, [Li(OEt_2)_3]^+ \\ X = Cl, I & & \mathbf{27} \\ & & \{Al_{12}[N(SiMe_3)_2]_8\}^{\bullet -} [Li(OEt_2)_3]^+ \\ & & \mathbf{28} \end{array} \qquad (12)$$

Besides structural aspects, the formation of metalloidal clusters is important for the understanding of the formation of bulk metals. This process of cluster formation as a first step on the reaction pathway to bulk metal is much more difficult to elucidate than the determination of geometrical structure. However, we were successful previously in finding two additional intermediates on the pathway from aluminum(I) to the $Al_{77}$ cluster. If a more reactive (compared to AlI) AlCl solution is combined with $LiN(SiMe_3)_2$ at low temperatures, **27** is obtained [44]. To the best of our knowledge **27** (Fig. 15) represents the first example in cluster chemistry, in which two $M_4$ tetrahedra (M = metal atom) are connected by a common corner, that means a ‘naked’ metal atom. In order to complete the coordination of this atom, similar to the coordination in metal, a planar six-membered Al ring is missing between the two $(AlR)_3$ rings. **27** may present a well-defined example for a single atom contact in nanophysics [47]. The next intermediate on the way to the $Al_{77}$ cluster is the $Al_{12}$ species **28** [48]. This radical anion (Fig. 16) is structurally analogous to the recently published neutral $In_{12}R_8$ ($R = Si^tBu_3$) [49]. Both species exhibit sections of the cubic close packed structures of metals.

Obviously, AlX solutions are powerful starting materials for the preparation of metalloidal clusters. Furthermore, these solutions also open the way to binary

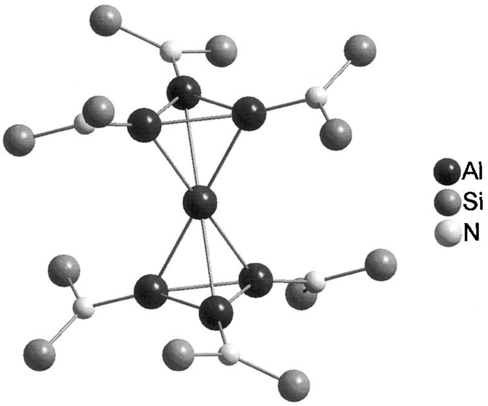

Fig. 15. View of a molecule of **27**.

clusters: If **13** is treated with AlCl and $SiCl_4$ or if $Sicp_2^*$ is allowed to react with AlCl solutions a $SiAl_{14}$ cluster **29** is formed (Fig. 17) [50]. Here a silicon atom centers a cube of eight aluminum atoms. Six Alcp* units reside on the faces of this cube. Surprisingly, this molecular cluster with an unique coordination of the central silicon atom can be vaporized and subsequently detected by mass spectroscopy. This stability of **29** can be understood by its special electronic structure, which fulfills the jellium model [51].

## 4.2. Gallium

The reaction of ultrasonic prepared gallium(I) iodide with hypersilyl lithium allowed the isolation of **18** only in low yields, whilst **21a** and **22** are the only detectable products in the analogous reactions of that gallium(I) iodide with the metallated trisyl $C(SiMe_3)_3$ and supersilyl $Si(^tBu)_3$ ligands (Eq. (13)) [52]. On the

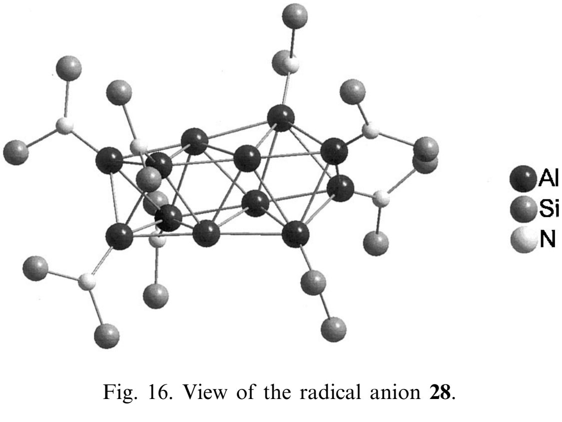

Fig. 16. View of the radical anion **28**.

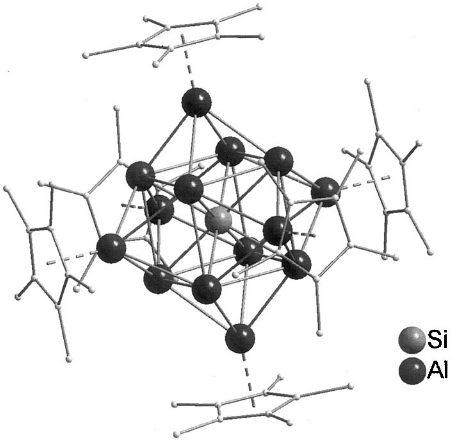

Fig. 17. View of a molecule of **29**.

other hand, with hypersilyl lithium the products of disproportionation **30**, **31**, and **32** are additionally observed, but with no liberation of gallium metal. Hence, products where gallium exists in an oxidation state lower than one are expected. This was confirmed by the isolation of the anionic $Ga_9$ cluster **33** · Li(thf)$_4$ (Eq. (14)) [53]. Here, seven gallium atoms form a slightly distorted pentagonal bipyramid (Fig. 18), which is bridged on two adjacent edges by hypersilyl gallium fragments. Thus, only six gallium atoms bear hypersilyl groups, the remaining three form only bonds to other gallium atoms. For the pentagonal bipyramidal $Ga_7$ part, eight cluster-binding electron pairs are available, such that **33** is a *closo* cluster agreement with the Wade–Williams–Rudolph rules [54]. The Ga–Ga distances range from 234.4 to 289.8 pm, thus covering the whole range of known Ga–Ga bond lengths.

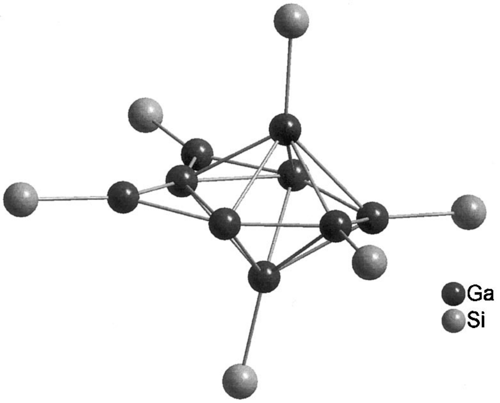

Fig. 18. View of the cluster anion of **33** · Li(thf)$_4$; methyl groups are omitted for clarity.

$GaI + RM \longrightarrow Ga_4R_4$

$M = Na, R = Si\mathit{t}Bu_3$ **22**

$M = Li,\ R = C(SiMe_3)_3$ **21a** (13)

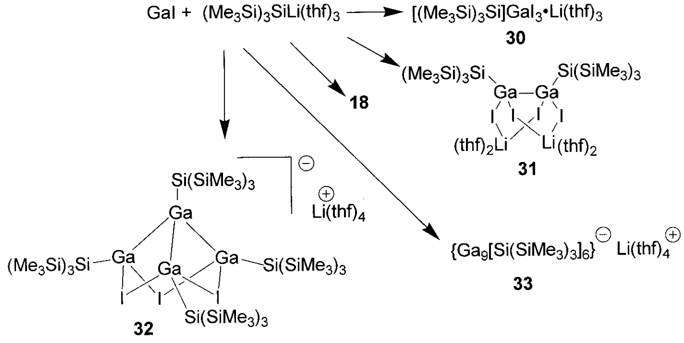

(14)

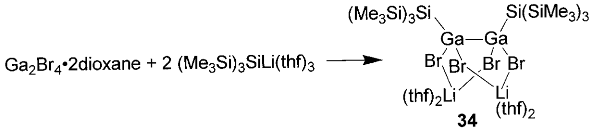

(15)

Complex **32** is a unique example of an electron precise tetragallane (Fig. 19), with a tetrahedral backbone of gallium atoms. Three edges are bridged by iodine atoms. Thus, **32** can be described as a heterocubane with one unoccupied corner. **31** is an ionic digallane derivative; its bromine analogue **34** (Fig. 20) is easily obtained from $Ga_2Br_4 \cdot 2$ dioxane and hypersilyl lithium (Eq. (15)) [52]. The similar reaction of

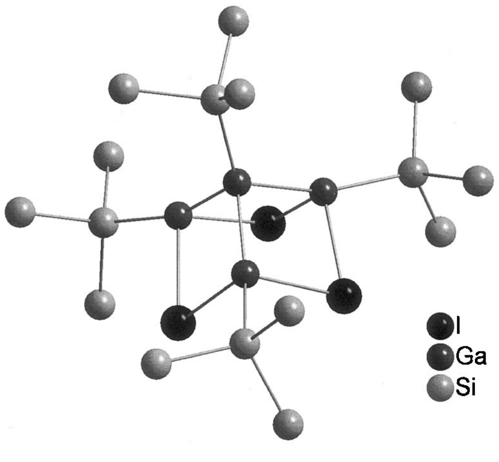

Fig. 19. View of the cluster anion of $\mathbf{32} \cdot Li(thf)_4$; methyl groups are omitted for clarity.

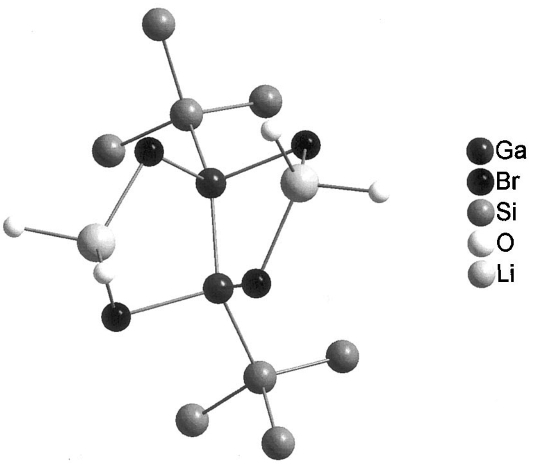

Fig. 20. View of a molecule of **34**; methyl groups are omitted for clarity.

$Ga_2Cl_4 \cdot 2$ dioxane and hypersilyl lithium (Eq. (16)) affords **3**, with a $Ga_4Cl_4$ cage comparable to the Realgar structure (Fig. 21) [55]. In some cases, i.e. if $Ga_2I_3$ or $Ga_2X_4 \cdot 2$ dioxane in THF are reacted with three or four equivalents of hypersilyl lithium the hypersilyl group is cleaved and acts as a source for $Si(SiMe_3)_2$ fragments in gallium silicon heterocyclic compounds **36** and **37** (Eq. (17)), Fig. 22) [56] and for $Si(SiMe_3)$ fragments in the *closo* polyhedral silagallane **38** (Eq. (18), Fig. 23) [57].

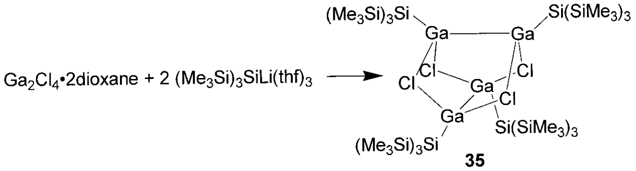

**35**

(16)

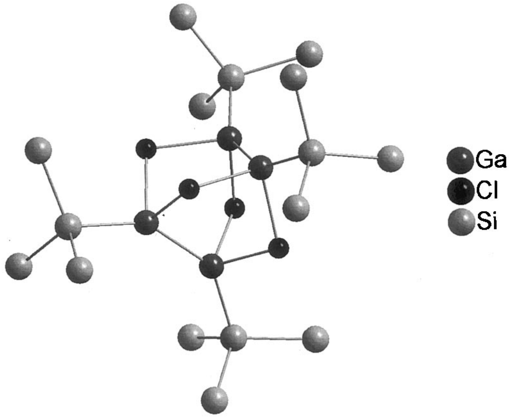

Fig. 21. View of a molecule of **35**; methyl groups are omitted for clarity.

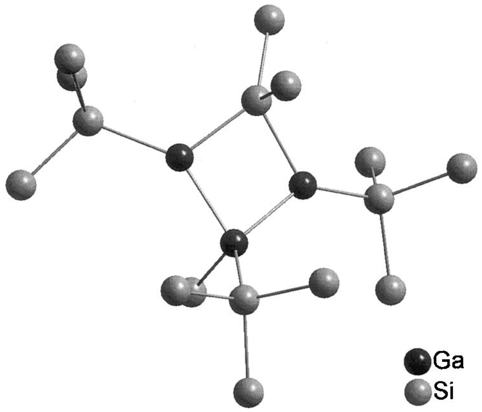

Fig. 22. View of the anion of **37** · Li(thf)$_4$; methyl groups are omitted for clarity.

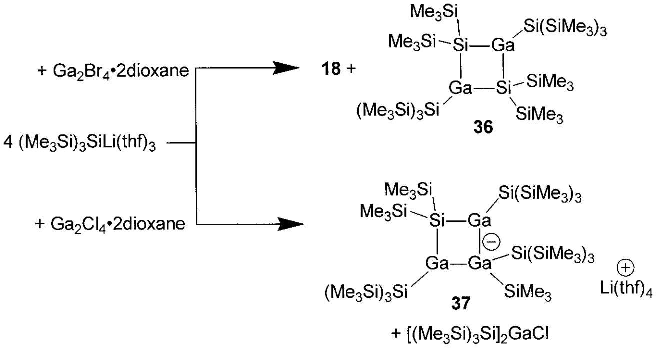

(17)

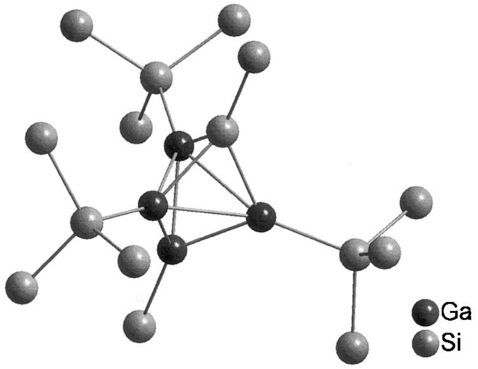

Fig. 23. View of the cluster anion of **38** · Li(thf)$_4$; methyl groups are omitted for clarity.

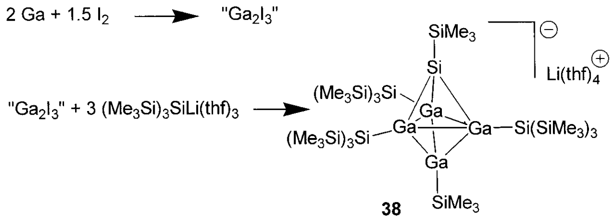

**38**

(18)

Complex **39**, the largest metal centered neutral metalloidal cluster so far, is obtained from GaBr solutions, which are more reactive than GaI, and hypersilyl lithium (Eq. (19)) [58]. Here a central gallium atom is surrounded by 13 gallium atoms. The usual coordination number of 12 in metals, which can be described as a cuboctahedral sequence of three parallel ring systems ($M_3$–$M_6$–$M_3$) is changed for **39** into the sequence $M_3$–$M_6$–$M_4$. Eight hypersilyl gallium groups are attached to four-membered ring facets of this $Ga_{13}$ shell (Fig. 24).

If $Li(thf)_3Ge(SiMe_3)_3$ is allowed to react with GaI instead of hypersilyl lithium (Eq. (20)), **4** — isomorphous to **39** — is isolated in good yield [59]. **39** and **40** are impressive examples of metalloidal clusters, because there are only eight Ga–Si/Ga–Ge bonds, but a large number of direct Ga–Ga contacts. Besides the $Ga_{22}$ core the overall compositions are remarkable: $Ga_{22}Si_{32}(CH_3)_{72}$ and $Ga_{22}Ge_8Si_{24}(CH_3)_{72}$, respectively. That is, the metalloidal core is surrounded by a 'shell' of 32 'semimetal' atoms and this entity is protected against the formation of bulk material by an organic shell of 72 methyl groups.

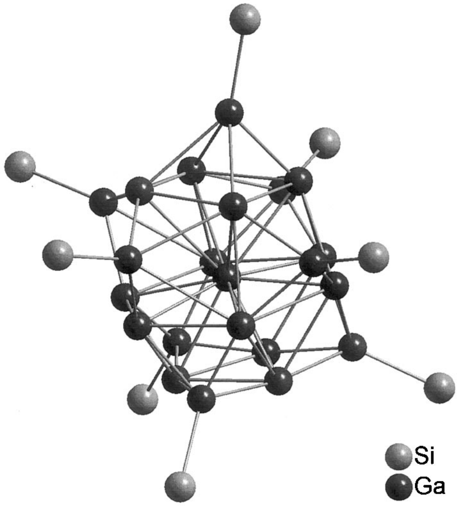

Fig. 24. View of a molecule of **39**.

$$\begin{aligned}&\mathrm{GaBr} + (\mathrm{Me_3Si})_3\mathrm{SiLi(thf)_3}\\ &\rightarrow [(\mathrm{Me_3Si})_3\mathrm{Si}]_2\mathrm{GaBr_2}\cdot\mathrm{Li(THF)_2} + [(\mathrm{Me_3Si})_3\mathrm{SiGaBr}]_4 + \underset{\mathbf{39}}{\mathrm{Ga_{22}[Si(SiMe_3)_3]_8}}\end{aligned} \tag{19}$$

$$\begin{aligned}&\mathrm{GaI} + (\mathrm{Me_3Si})_3\mathrm{GeLi(thf)_3}\\ &\rightarrow [(\mathrm{Me_3Si})_3\mathrm{Ge}]_2\mathrm{GaI_2}\cdot\mathrm{Li(THF)_2} + \underset{\mathbf{40}}{\mathrm{Ga_{22}[Ge(SiMe_3)_3]_8}}\end{aligned} \tag{20}$$

To summarize this chapter, Al(I) and Ga(I) halides are especially powerful starting materials for the novel class of metalloidal clusters, most of which could be characterized by X-ray crystallography. Therefore these clusters provide for the first time a detailed insight into the geometric arrangement of species containing metal atoms, which are surrounded only by further metal atoms. Here a boundary is approached, where larger molecular clusters are on the pathway to bulk metals.

## 5. ER fragments as ligands in transition metal complexes

The coordination chemistry of aluminum, gallium and indium to transition metal fragments has been recently reviewed [60], so we will confine ourselves to the coordination of ER (E = Al, Ga) compounds. Due to their lone pair these organyl aluminum and gallium fragments are expected to behave as complex ligands. Formally, they may be regarded as CO analogues, as they possess two empty $\pi$ orbitals. Consequently, similar coordination modes — terminal and bridging — are possible.

In principle, two synthetic routes to RE–transition metal complexes have been used: The substitution of loosely bonded ligands by monovalent aluminum and gallium compounds. All examples published so far are discussed in Section 5.1. The second method is via salt elimination between divalent metal carbonylates $[\mathrm{M(CO)}_n]^{2-}$ and aluminum or gallium halide derivatives. The first results based on

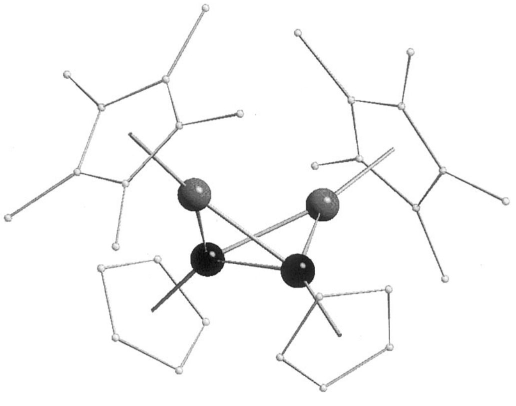

Fig. 25. View of a molecule of **41**.

this method have already been published 20 years ago [61]. Further examples are discussed in Section 5.2.

### *5.1. Ligand substitution by Alcp*, Gacp* and similar reactions*

The first reaction, in which Alcp* was used in order to form transition metal complexes was described in 1994. **41** with a 'butterfly' structure (Fig. 25) was obtained from $Nicp_2$ and Alcp* (Scheme 2) [62]. Later on, many other similar reactions were performed to obtain complexes **42** [63], **43**, and **44** [27] with the Ecp* fragments as terminal ligands (Fig. 26). This kind of substitution is also possible with other ligands, as was demonstrated by the reaction between a gallium(I) phosphol and $(C_8H_{14})Cr(CO)_5$ (Eq. (21)) affording **45** (Fig. 27) [64], and by the

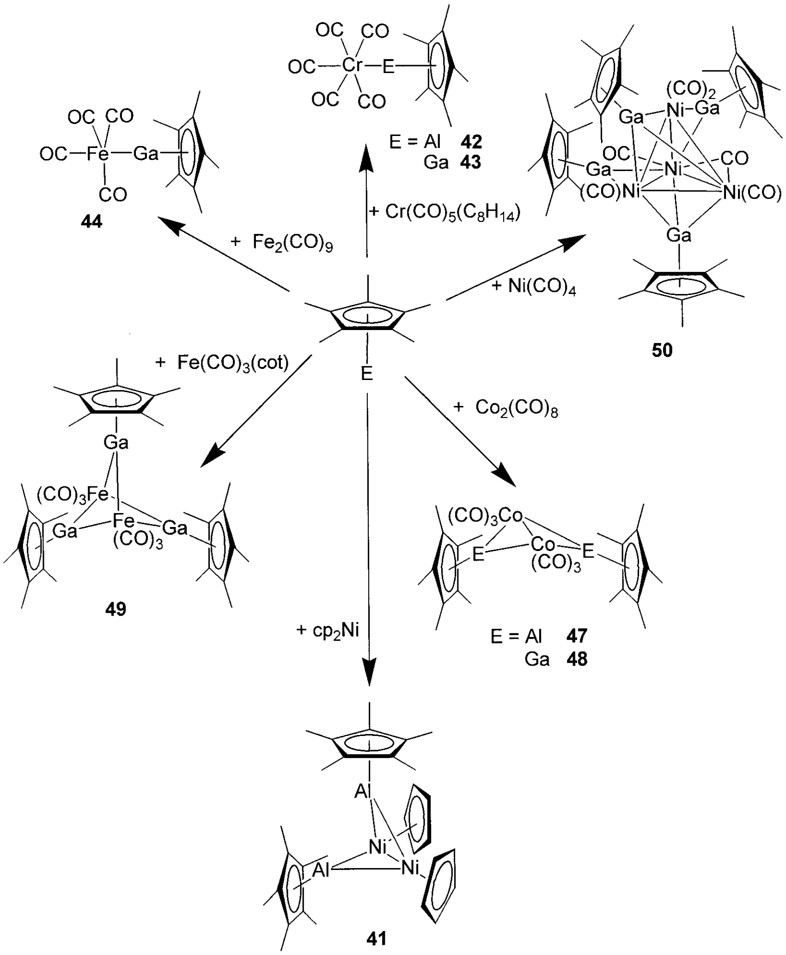

Scheme 2.

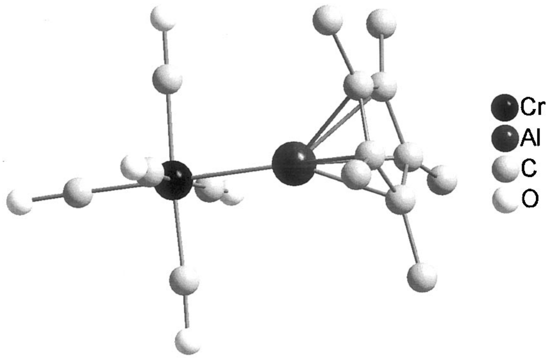

Fig. 26. View of a molecule of **42**, **43** and **44**.

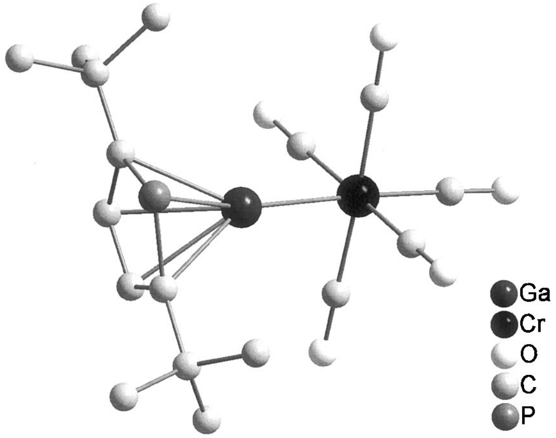

Fig. 27. View of a molecule of **45**.

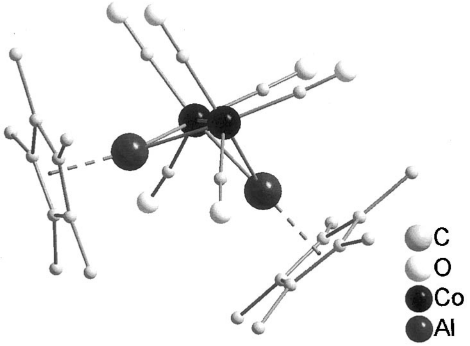

Fig. 28. View of a molecule of **47**.

synthesis of the fascinating homoleptic $Ni(ER)_4$ compounds **46a** [65] and **b** [66] (E = Ga, In) from the tetrahedranes **21a** and $Ni(cod)_2$ (Eq. (22)). By ligand displacement reactions the dinuclear cluster compounds **47** (Fig. 28) [67], **48** and **49** [27] are also available. The remarkable $Ni_4Ga_4$ cluster **50** contains $\mu_2$- and $\mu_3$-Gacp* ligands [27].

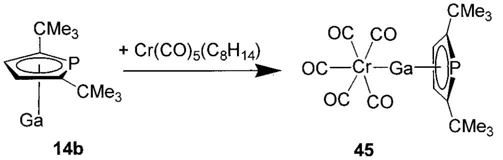

**14b** **45** (21)

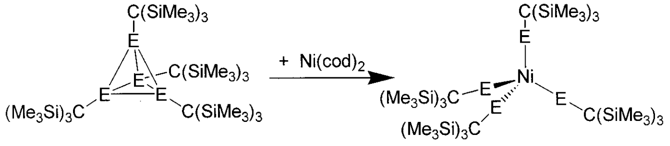

E = Ga **46a**
In **46b** (22)

## *5.2. Carbonylates as starting materials*

From the reaction of $[M(CO)_n]^{2-}$ (M = Fe, Cr) with $REX_2$ compounds (R = Cl, $CH_3$ and $C_2H_5$) dimeric **51** [61] (Eq. (23)) as well as complexes with terminal $ER(L_2)$ ligands **52** [66] could be isolated in the presence of Lewis bases (Eq. (24)). With more bulky substituents (pyrazolylborate, cp*, and aryl*) complexes **53** [69], **54**, [70] and **55** [71a] with terminal ER groups are accessible (Eq. (25)).

In Table 4 Ga–Fe bond lengths and CO stretching frequencies of some Ga–$Fe(CO)_4$ species are mentioned.

Table 4
Compounds with different substituted terminal Ga fragments bonded to a $Fe(CO)_4$ entities: CO stretching modes and Fe–Ga bond distances (experimental and calculated data)

| Compound | | $d_{Fe-Ga}$ (pm) | CO stretching modes ($cm^{-1}$) | Refs. |
|---|---|---|---|---|
| tmeda(Cl)Ga–$Fe(CO)_4$ | **52c** | 233.8(2) | 2011, 1928, 1881 | [68] |
| $HB(Me_2pyr)_3$Ga–$Fe(CO)_4$ | **53** | 231.5(3) | 2008, 1926, 1878 | [69] |
| aryl*Ga–$Fe(CO)_4$ | **55** | 222.48(7) | 2032, 1959, 1941, 1929 | [71a] |
| $[(CO)_4Fe–Ga\{Fe_3(CO)_9–[GaSi(SiMe_3)_3]_2\}]^-$ | **61** | 228.9(1) | – | [72] |
| cp*Ga–$Fe(CO)_4$ | **49** | 227.3(1) | 2037, 1966, 1942 | [27] |
| cpGa–$Fe(CO)_4$ (calc.) | | 232.7 | 2040, 1983, 1959 | [73] |
| $C_6H_5$Ga–$Fe(CO)_4$ (calc.) | | 225.6 | 2038, 1985, 1960, 1958 | [73] |
| HGa–$Fe(CO)_4$ (calc.) | | 220.0 | – | [72] |

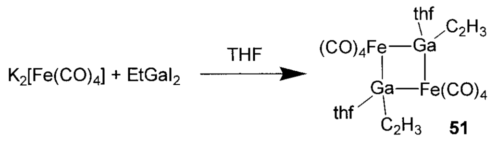

(23)

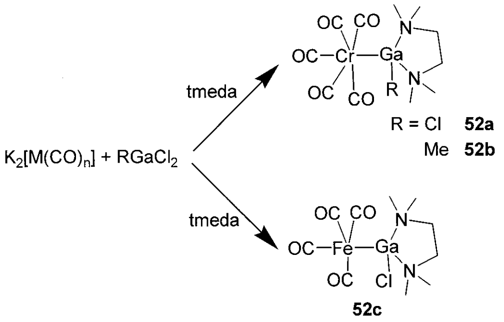

(24)

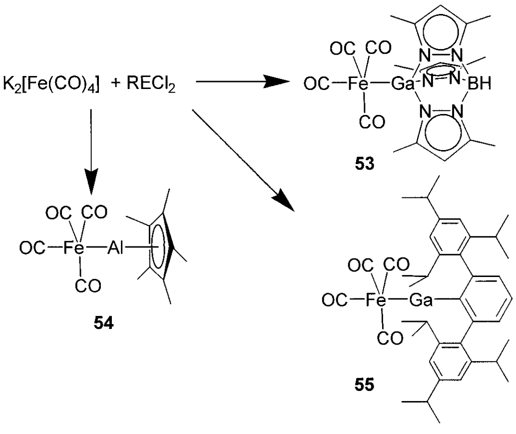

(25)

Starting from the dimeric digallane **35** and divalent carbonylferrates (Scheme 3) a series of gallium iron clusters is accessible [72], which all exhibit bridging $(Me_3Si)_3SiGa$ groups replacing three (**56**), two (**57**), or only one (**58**) bridging CO ligand in $Fe_2(CO)_9$ (Figs. 29 and 30). **59** (Fig. 31) is the sodium chloride adduct of **57**, thus showing the remaining Lewis acidity of bridging RGa ligands. Furthermore, two cluster compounds with a $Ga_2Fe_3$ core are obtained from these reactions; in **60** (Fig. 32) two gallium atoms are in the apical position of a trigonal bipyramid, in the equatorial plane three $Fe(CO)_3$ fragments complete the anionic polyhedron. One iron–iron edge is bridged by a hydrogen atom. Thus, a *Wade*-type *closo* cluster with six cluster-binding electron pairs results of the same type as **61** (Fig. 33). Here, the bridging hydrogen is replaced by a $GaFe(CO)_4$ group.

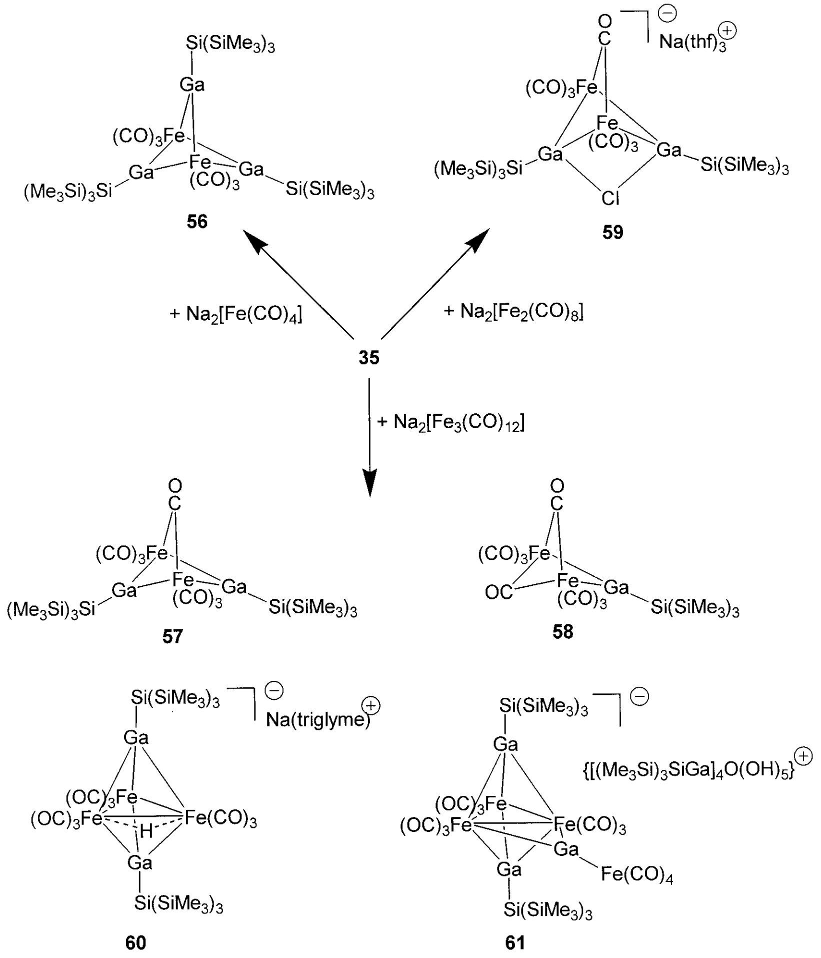

Scheme 3.

## 5.3. Bonding of GaR and AlR ligands within transition metal complexes

The first hint for multiple bonding between transition metal fragments and AlR or GaR ligands, respectively, [71a] has led to considerable controversy [71b]. The whole literature about this subject is mentioned in the latest paper of Frenking, in which a critical discussion on the basis of DFT calculations is presented [73]. We don't want to repeat the arguments for and against M–Ga/Al multiple bonding, however, we want to ask a theoretical question: What are the criteria for a bond? Are arguments deduced from theory or from experiment essential? Of course there

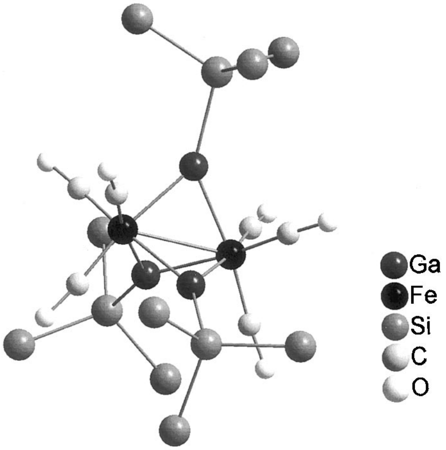

Fig. 29. View of a molecule of **56**.

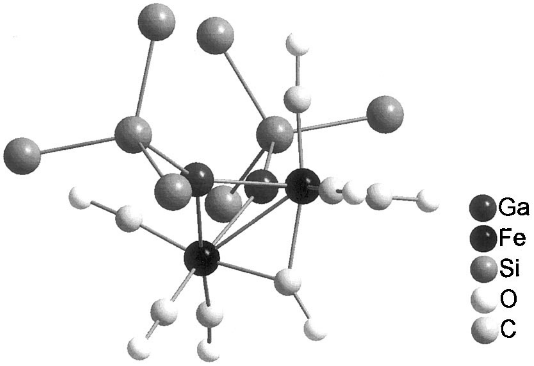

Fig. 30. View of a molecule of **57**.

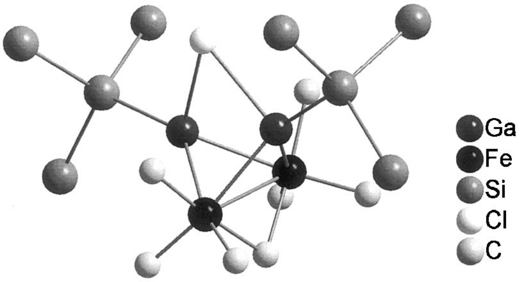

Fig. 31. View of a molecule of **59**.

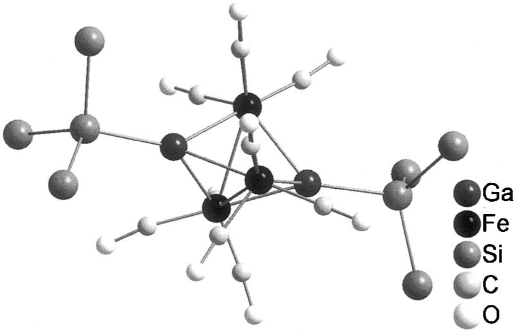

Fig. 32. View of the cluster anion of **60** · Na(triglyme); Si-methyl groups are omitted for clarity.

are no problems if theory confirms the experimental data. Since we have the feeling, that in the case of M–GaR/M–AlR bonding theoretical aspects have so far been overestimated (Section 2.1), we want to discuss this problem more on the basis of observable data. However, since these data are often difficult to obtain, we also use quantum chemical calculations for this purpose [9]. In the following discussion we will concentrate on AlR species instead of GaR species and as a transition metal fragment we chose the $Fe(CO)_4$ entity [8].

First of all we have a look at the following reaction:

$$Fe(CO)_5 + AlCp \rightarrow (OC)_4FeAlCp + CO \quad \Delta E = -23\ kJ\ mol^{-1}$$

The exothermic character (from DFT calculations) of this reaction tells us that Fe–C and Fe–Al bonding do not differ in principle. There is only a quantitative

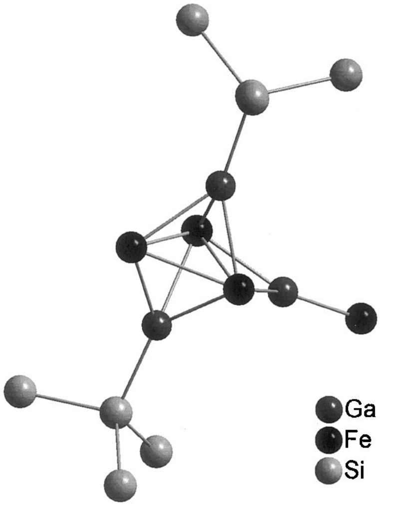

Fig. 33. View of the cluster anion of **61** · $[Ga(hypersilyl)]_4O(OH)_5$; methyl and CO groups are omitted for clarity.

difference concerning the polarity of these bonds [67], which is plausible since AlR species are stronger reducing agents than CO. With respect to polarity the Fe–Al bond in $(OC)_4FeAlCp$ and the Fe–Si bond in a hypothetical $(OC)_4FeSiO$ species are just between Fe–CO bonding in $Fe(CO)_5$ and that in $Fe(CO)_4^{2-}Na^{2+}$. For $Fe(CO)_4^{2-}$ reduction is completed and therefore nobody will describe $Na_2Fe(CO)_4$ as a stabilization product of Na atoms [74].

The discussion of Fe–Al bonding on the basis of redox-chemistry is also reflected by the charges from population analyses, which impressively show that, e.g. the Al atom in $(OC)_4FeAlCp$ is very similar to that in the typical $Al^{3+}$ compound $[cp_2^*Al]^+$ [67]. The polar Al–Fe bonding is also in line with a further description: $Fe(CO)_4^{2-}$ is isolobal with $O^{2-}$ and therefore from the point of view of the Al atom $(OC)_4FeAlCp$ may be compared with O=Al–Cp*. DFT calculations now show, that the Al atoms carry a high positive charge in both cases $(+0.7/+0.42)$ [67]. Unequivocally the Al atoms in O=AlCp have an oxidation number of +III. However, the question about the amount of covalent, multiple bonding remains. To answer this question we want to introduce the force constant as an observable, which seems to be the most appropriate molecular constant (Section 2.1). In order to get an experimentally determined value for an Al=O double bond, we have to look at the matrix isolated molecules O=AlF and O=AlCl [76], which are to the best of our knowledge the only examples of an Al=O double bond. The measured Al–O force constant is 6.6 mdyn $Å^{-1}$ [76] which marks a double bond weakened by polar contributions, since for a typical Al–O single bond a value of 4.2 mdyn $Å^{-1}$ has been obtained [77]. From these experimental findings one can conclude a similar Fe–Al double bond e.g. in $(OC)_4FeAlCp^*$.

Since, as mentioned above, CO and AlR show similar behavior as ligands, then it also follows that CO forms double bonds with transition metal fragments. This bonding scheme is supported by additional results.

The simplest species containing a transition metal atom and a carbene like ligand are, e.g. molecules like PdCO and PdSiO [78]. Both complexes have been investigated via a matrix isolation technique. In addition we have calculated some molecular constants for similar species PdAlF, PdAlH and PdAlCp [8,9]. Besides the PdX force constants the distances and the calculated charges are summarized in Table 5.

Table 5
Calculated [8,9] force constants $f$ (mdyn $Å^{-1}$), distances $d$ (pm) and charges $Q$ (Mulliken) for some PdXY species (experimental results are given in brackets [78,79])

| | $f$(PdX) | $f$(XY) | $f'$(PdX/XY) | $d$(PdX) | $Q$(Pd) |
|---|---|---|---|---|---|
| PdCO | 3.65 | 16.78 (16.97) | 0.49 | 183 | 0.05 |
| PdSiO | 2.68 | 8.39 | 0.06 | 213 | −0.05 |
| | (2.69) | (8.92) | 0.0 | | |
| PdAlF | 2.21 | 4.45 | 0.00 | 219 | −0.12 |
| PdAlH | 2.26 | 1.79 | −0.01 | 220 | −0.14 |
| PdAlCp | 2.00 | | | 221 | −0.33 |

Table 6
Calculated [8,9] distances d (pm), charges $Q$ (Mulliken), CO frequencies $\nu$ ($cm^{-1}$) and $\Delta E$ (kJ $mol^{-1}$) for the reaction: $PdCO + XY \rightarrow YXPdCO$

| | $d$(PdX) | $d$(PdC) | $Q$(Pd) | $Q$(CO) | $Q$(X) | $\nu$(CO) | $\Delta E$ |
|---|---|---|---|---|---|---|---|
| OCPdCO | 193.7 | 193.7 | −0.39 | 0.2 | 0.14 | 2062/2139 | −164 |
| OCPdSiO | 225.5 | 196.2 | −0.35 | 0.14 | 0.54 | 2100 | −137 |
| OCPdAlF | 236.0 | 193.7 | −0.31 | 0.08 | 0.55 | 2076 | −139 |
| OCPdAlCp | 241.2 | 190.9 | −0.48 | 0.05 | 0.45 | 2049 | −155 |

Surprisingly, these force constants are much larger than, e.g. the Ga–Ga force constants mentioned in the beginning (see Table 1). With respect to an old fashioned estimation [80,81] these bonds may be regarded as weak double bonds, which is a further confirmation for the above mentioned postulation of double bonding between the transition metal and the Al/Ga–atom [82].

There is a further very classical way to get information about M–X bonding: the frequency shift of the CO stretching motion of CO ligands, which are connected to the same transition metal atoms. We chose a very simple system, for which experimental results [78,79] can be easily completed by DFT calculations. The results for OCPdX (X = CO, SiO, AlF, AlCp) are summarized in Table 6.

With respect to the PdX dissociation energy there is no remarkable difference between CO and AlCp, which is further confirmation for our above-mentioned hypothesis of an M–Al double bond. However, as expected there are differences in polarity, which are reflected in the charges and also in the changes of the CO frequencies. This means, in general the detection of CO frequencies gives a useful hint for differences in transition metal–X bonding, although it has recently been shown that this procedure is not appropriate in any case [73].

To sum up, in order to make progress in the discussion of Ga–Ga and M–Ga/Al bonding we would strongly suggest to concentrate more on force constants as observables, though they are difficult to measure and also to calculate. Already the nomenclature of force constants tells us that forces are involved, which resist the elongation of bonds. In a very descriptive way this elastic spring force reflects the strength of a bond much better than the occupation of orbitals to which a bonding or a non-bonding character cannot be unequivocally attributed. Therefore we state once more, look more carefully onto experimental findings than onto the occupation of certain MOs. That is, more compounds like $(CO)_4Fe$–AlR/–GaR have to be prepared and to be investigated (e.g. structure and spectroscopy). In the near future, on the basis of these results and with the help of quantum chemical calculations it should be possible to get a better understanding of this unusual (or usual) bonding in Ga–Ga and M–GaR/–AlR systems.

## Acknowledgements

We thank the Deutsche Forschungsgemeinschaft for financial support and R. Köppe, W. Köstler, A. Purath, G. Stößer, and C. Üffing for helpful discussions.

## References

[1] (a) W. Uhl, Angew. Chem. 105 (1993) 1449; Angew. Chem. Int. Ed. Engl. 32 (1993) 1386. (b) W. Uhl, Coord. Chem. Rev. 163 (1997) 1.

[2] W. Hiller, K.-W. Klinkhammer, W. Uhl, J. Wagner, Angew. Chem. 103 (1991) 182; Angew. Chem. Int. Ed. Engl. 30 (1991) 179.

[3] J. Su, X.-W. Li, R.C. Crittendon, G.H. Robinson, J. Am. Chem. Soc. 119 (1997) 5471.

[4] (a) X.-W. Li, W.T. Pennington, G.H. Robinson, J. Am. Chem. Soc. 117 (1995) 7578. (b) X.-W. Li, Y. Xie, P.R. Schreiner, K.D. Gripper, R.C. Crittendon, C.F. Campana, H.F. Schaefer, G.H. Robinson, Organometallics 15 (1996) 3798.

[5] N. Wiberg, K. Amelunxen, H. Nöth, H. Schwenk, W. Kaim, A. Klein, T. Scheiring, Angew. Chem. 109 (1997) 1258; Angew. Chem. Int. Ed. Engl. 36 (1997) 1213.

[6] (a) M.M. Olmstead, R.S. Simons, P.P. Power, J. Am. Chem. Soc. 119 (1997) 11705. (b) F.A. Cotton, A.H. Cowley, X. Feng, J. Am. Chem. Soc. 120 (1998) 1795. (c) R. Dagani, Chem. Eng. News 75 (1997) 9.

[7] (a) Y. Xie, R.S. Grev, J. Gu, H.F.S. Schaefer III, P. von R. Schleyer, J. Su, X.-W. Li, G.H. Robinson, J. Am. Chem. Soc. 120 (1998) 3773. (b) K.-W. Klinkhammer, Angew. Chem. 109 (1997) 2414; Angew. Chem. Int. Ed. Engl. 36 (1997) 2320. (c) In the special case of **4**, interactions between the aromatic ligands and the $Na^+$ cations contribute to the reduction of the Ga–Ga distance [6b].

[8] R. Köppe, H. Schnöckel, Z. Anorg. Allg. Chem. 626 (2000) 1095.

[9] (a) RI-DFT calculations and TURBOMOLE program package: R. Ahlrichs, M. Bär, M. Häser, H. Horn, C. Kölmel, Chem. Phys. Lett. 162 (1989) 165. (b) O. Treutler, H. Öhm, M. Häser, R. Ahlrichs, Chem. Phys. Lett. 240 (1995) 283. (c) A. Schäfer, H. Horn, R. Ahlrichs, J. Chem. Phys. 97 (1992) 2751. (d) K. Eichkorn, O. Treutler, H. Ohm, M. Häser, R. Ahlrichs, Chem. Phys. Lett. 242 (1995) 652.

[10] (a) E.B. Wilson, Jr., J.C. Decius, P.C. Cross, Molecular Vibrations, The Theory of Infrared and Raman Vibrational Spectra; McGraw-Hill, New York, 1955. (b) We used a program obtained from Professor P. Pulay some years ago. (c) Perhaps the product between the distance and the force constant, which reflects a force may be a more suitable way to compare similar bonds.

[11] K.P. Huber, G. Herzberg, Molecular Spectra and Molecular Structure IV. Constants of Diatomic Molecules, Van Nostrand Reinhold, New York, 1979.

[12] (a) J.C. Beamish, R.W.H. Small, I.J. Worrall, Inorg. Chem. 18 (1979) 220. (b) K.L. Brown, D. Hall, J. Chem. Soc. Dalton Trans. (1973) 1843. (c) G. Gerlach, W. Hönle, A. Simon, Z. Anorg. Allg. Chem. 486 (1982) 7.

[13] M.L.H. Green, P. Mountford, G.J. Smout, S.R. Speel, Polyhedron 9 (1990) 2763.

[14] A. Schnepf, C. Doriat, E. Möllhausen, H. Schnöckel, Chem. Commun. (1997) 2111.

[15] M.C. Kuchta, J.B. Bonnano, G. Parkin, J. Am. Chem. Soc. 118 (1996) 10914.

[16] (a) M. Mocker, C. Robl, H. Schnöckel, Angew. Chem. 106 (1994) 946; Angew. Chem. Int. Ed. Engl. 33 (1994) 862. (b) A. Ecker, E. Baum, M.A. Friesen, R. Köppe, M.A. Junker, C. Üffing, H. Schnöckel, Z. Anorg. Allg. Chem. 624 (1998) 513.

[17] C. Dohmeier, D. Loos, H. Schnöckel, Angew. Chem. 108 (1996) 141; Angew. Chem. Int. Ed. Engl. 35 (1996) 129.

[18] M. Tacke, H. Schnöckel, Inorg. Chem. 28 (1989) 2895.

[19] D. Loos, H. Schnöckel, D. Fenske, Angew. Chem. 105 (1993) 1124; Angew. Chem. Int. Ed. Engl. 32 (1993) 1059.

[20] (a) M. Mocker, C. Robl, H. Schnöckel, Angew. Chem. 106 (1994) 1860; Angew. Chem. Int. Ed. 33 (1994) 1754. (b) A. Ecker, H. Schnöckel, Z. Anorg. Allg. Chem. 622 (1996) 149. (c) A. Ecker, H. Schnöckel, Z. Anorg. Allg. Chem. 624 (1998) 813.

[21] C.U. Doriat, E. Baum, A. Ecker, H. Schnöckel, Angew. Chem. 109 (1997) 2057; Angew. Chem. Int. Ed. Engl. 36 (1997) 1969.

[22] C. Klemp, R. Köppe, E. Weckert, H. Schnöckel, Angew. Chem. 111 (1999) 1852; Angew. Chem. Int. Ed. Engl. 38 (1999) 1740.

[23] C. Dohmeier, C. Robl, M. Tacke, H. Schnöckel, Angew. Chem. 103 (1991) 594; Angew. Chem. Int. Ed. Engl. 30 (1991) 564.

[24] S. Schulz, H.W. Roesky, H.J. Koch, G.M. Sheldrick, D. Stalke, M. Kuhn, Angew. Chem. 105 (1993) 1828; Angew. Chem. Int. Ed. Engl. 32 (1993) 1729.

[25] (a) D. Loos, H. Schnöckel, J. Organomet. Chem. 463 (1993) 37. (b) D. Loos, Dissertation, Universität München, 1994. (c) C. Doriat, Dissertation, Universität Karlsruhe (TH), 1998.

[26] D. Loos, H. Schnöckel, J. Gauss, U. Schneider, Angew. Chem. 104 (1992) 1376; Angew. Chem. Int. Ed. Engl. 31 (1992) 1362.

[27] P. Jutzi, B. Neumann, G. Reumann, H.-G. Stammler, Organometallics 17 (1998) 1305.

[28] (a) H. Sitzmann, M.F. Lappert, C. Dohmeier, C. Üffing, H. Schnöckel, J. Organomet. Chem. 561 (1998) 203. (b) For quantum chemical calculations see: U. Schneider, R. Ahlrichs, H. Horn, A. Schäfer, Angew. Chem. 104 (1992) 327; Angew. Chem. Int. Ed. Engl. 31 (1992) 353. (c)J. Gauss, U. Schneider, R. Ahlrichs, C. Dohmeier, H. Schnöckel, J. Am. Chem. Soc. 115 (1993) 2402.

[29] D. Loos, E. Baum, A. Ecker, H. Schnöckel, A.J. Downs, Angew. Chem. 109 (1997) 894; Angew. Chem. Int. Ed. Engl. 36 (1997) 861.

[30] O.T. Beachley Jr., R. Blom, M.R. Churchill, K. Faegri Jr., J.C. Fettinger, J.C. Pazik, L. Victoriano, Organometallics 8 (1989) 346.

[31] H. Werner, H. Otto, H.J. Kraus, J. Organomet. Chem. 315 (1986) C57.

[32] A. Haaland, K.-G. Martinsen, H.V. Volden, D. Loos, H. Schnöckel, Acta Chem. Scand. 48 (1994) 172.

[33] A. Purath, H. Schnöckel, J. Organomet. Chem. 579 (1999) 373.

[34] A. Purath, C. Dohmeier, A. Ecker, H. Schnöckel, K. Amelunxen, T. Passler, N. Wiberg, Organometallics 17 (1998) 1894.

[35] C. Schnitter, H.W. Roesky, C. Röpken, R. Herbst-Irmer, H.-G. Schmidt, M. Noltemeyer, Angew. Chem. 110 (1998) 2059; Angew. Chem. Int. Ed. Engl. 37 (1998) 1952.

[36] W. Uhl, W. Hiller, M. Layh, W. Schwarz, Angew. Chem. 104 (1992) 1378; Angew. Chem. Int. Ed. Engl. 31 (1992) 1364.

[37] G. Linti, J. Organomet. Chem. 520 (1996) 107.

[38] W. Uhl, J. Organomet. Chem. 555 (1998) 263.

[39] N. Wiberg, Coord. Chem. Rev. 163 (1997) 217.

[40] A. Haaland, K.-G. Martinsen, H.V. Volden, W. Kaim, E. Waldhör, W. Uhl, U. Schütz, Organometallics 15 (1996) 1146.

[41] C.K.F. von Hänisch, C. Üffing, M.A. Junker, A. Ecker, B.O. Kneisel, H. Schnöckel, Angew. Chem. 108 (1996) 3003; Angew. Chem. Int. Ed. Engl. 35 (1996) 2875.

[42] C. Üffing, E. Baum, R. Köppe, H. Schnöckel, Angew. Chem. 110 (1998) 2488; Angew. Chem. Int. Ed. Engl. 37 (1998) 2397.

[43] C. Dohmeier, M. Mocker, H. Schnöckel, A. Lötz, U. Schneider, R. Ahlrichs, Angew. Chem. 105 (1993) 1491; Angew. Chem. Int. Ed. Engl. 32 (1993) 1428.

[44] A. Purath, R. Köppe, H. Schnöckel, Angew. Chem. 111 (1999) 3114; Angew. Chem. Int. Ed. 38 (1999) 2926.

[45] A. Ecker, E. Weckert, H. Schnöckel, Nature 387 (1997) 379.

[46] N.T. Tran, M. Kawano, D.R. Powell, L.F. Dahl, J. Am. Chem. Soc. 120 (1998) 10986, and references therein.

[47] E. Scheer, N. Agrait, J.C. Cuevas, L.A. Yeyati, B. Ludoph, A. Martin-Rodero, G.R. Bollinger, J.M. van Ruitenbeek, C. Urbina, Nature 394 (1998) 154.

[48] A. Purath, R. Köppe, H. Schnöckel, Chem. Commun. (1999) 1933.

[49] N. Wiberg, T. Blank, H. Nöth, W. Ponikwar, Angew. Chem. 111 (1999) 887; Angew. Chem. Int. Ed. Engl. 38 (1999) 839.

[50] A. Purath, C. Dohmeier, A. Ecker, R. Köppe, H. Krautscheid, H. Schnöckel, R. Ahlrichs, C. Stoermer, J. Friedrich, P. Jutzi, J. Am. Chem. Soc., accepted for publication.

[51] W.D. Knight, K. Clemenger, W.A. de Heer, W. Saunders, M.Y. Chau, M.L. Cohen, Phys. Rev. Lett. 52 (1984) 2124.

[52] G. Linti, A. Rodig, unpublished results.

[53] G. Linti, W. Köstler, Angew. Chem. 109 (1997) 2758; Angew. Chem. Int. Ed. Engl. 36 (1997) 2644.

[54] (a) K. Wade, Adv. Inorg. Radiochem. 18 (1976) 1. (b) R.E. Williams, Adv. Inorg. Radiochem. 18 (1976) 67.

[55] G. Linti, W. Köstler, Angew. Chem. 108 (1996) 593; Angew. Chem. Int. Ed. Engl. 35 (1996) 550.
[56] G. Linti, W. Köstler, A. Rodig, Eur. J. Inorg. Chem. 1 (1998) 745.
[57] G. Linti, W. Köstler, H. Piotrowski, A. Rodig, Angew. Chem. 110 (1998) 2331; Angew. Chem. Int. Ed. Engl. 37 (1998) 2209.
[58] A. Schnepf, E. Weckert, G. Linti, H. Schnöckel, Angew. Chem. 111 (1999) 3578; Angew. Chem. Int. Ed. Engl. 38 (1999) 3381.
[59] G. Linti, A. Rodig, Chem. Commun. (2000) 127.
[60] R.A. Fischer, J. Weiß; Angew. Chem. 111 (1999) 3002, Angew. Chem. Int. Ed. Engl. 38 (1999) 2830.
[61] J.C. Vanderhooft, R.D. Ernst, F.W. Cagle Jr., R.J. Neustadt, T.H. Cymbaluk, Inorg. Chem. 21 (1982) 1876.
[62] C. Dohmeier, H. Krautscheid, H. Schnöckel, Angew. Chem. 106 (1994) 2570; Angew. Chem. Int. Ed. Engl. 33 (1994) 2482.
[63] Q. Yu, A. Purath, A. Donchev, H. Schnöckel, J. Organomet. Chem. 584 (1999) 94.
[64] A. Schnepf, G. Stößer, D. Carmichael, F. Mathey, H. Schnöckel, Angew. Chem. 111 (1999) 1757; Angew. Chem. Int. Ed. Engl. 38 (1999) 1646.
[65] W. Uhl, M. Benter, S. Melle, W. Saak, G. Frenking, J. Uddin, Organometallics 18 (1999) 3778.
[66] W. Uhl, M. Pohlmann, R. Wartchow, Angew. Chem. 110 (1998) 1007; Angew. Chem. Int. Ed. Engl. 37 (1998) 961.
[67] C. Üffing, A. Ecker, R. Köppe, H. Schnöckel, Organometallics 17 (1998) 2373.
[68] (a) M.M. Schulte, E. Herdtweck, G. Raudaschl-Sieber, R.A. Fischer, Angew. Chem. 108 (1996) 489; Angew. Chem. Int. Ed. Engl. 35 (1996) 424. (b) R.A. Fischer, M.M. Schulte, J. Weiß, L. Zsolnai, A. Jacobi, G. Huttner, G. Frenking, C. Boehme, S.F. Vyboishchikov, J. Am. Chem. Soc. 120 (1998) 1237.
[69] (a) D.L. Reger, D.G. Garza, A.L. Rheingold, G.P.A. Yap, Organometallics 17 (1998) 3624. (b) Indium analogue: D.L. Reger, S.S. Mason, A.L. Rheingold, B.S. Haggerty, F.P. Arnold, Organometallics 13 (1994) 5049.
[70] J. Weiß, D. Stetzkamp, B. Nuber, R.A. Fischer, C. Boehme, G. Frenking, Angew. Chem. 109 (1997) 95; Angew. Chem. Int. Ed. Engl. 36 (1997) 70.
[71] (a) J. Su, X.-W. Li, R.C. Crittendon, C.F. Campana, G.H. Robinson, Organometallics 16 (1997) 4511. (b) F.A. Cotton, X. Feng, Organometallics 17 (1998) 128.
[72] G. Linti, W. Köstler, Chem. Eur. J. 4 (1998) 942.
[73] G. Frenking, C. Boehme, Chem. Eur. J. 5 (1999) 2184.
[74] Because the $Fe(CO)_4$ fragment in $(OC)_4FeAlR$ is a reduced species its Fe–Al bonding is completely different from that in $O{=}M(CO)_n$ species, in which the transition metal is oxidized. For these O=M bonds a triple bond has been discussed and incorrectly compared with the situation in FeAl or FeGa species [73,75].
[75] A. Neuhaus, A. Veldkamp, G. Frenking, Inorg. Chem. 33 (1994) 5278.
[76] H. Schnöckel, J. Mol. Struct. 50 (1978) 267.
[77] R. Ahlrichs, L. Zhengyan, H. Schnöckel, Z. Anorg. Allg. Chem. 519 (1984) 155.
[78] T. Mehner, R. Köppe, H. Schnöckel, Angew. Chem. 104 (1992) 653; Angew. Chem. Int. Ed. Engl. 31 (1992) 638.
[79] E.P. Kündig, M. Moskovits, G.A. Ozin, Can. J. Chem. 50 (1972) 3587.
[80] Siebert has estimated single bond strengths and got the following values (mdyn $Å^{-1}$), e.g. for $f(\text{Pd–CO}) = 1.98$; $f(\text{Pd–Si}) = 1.37$; $f(\text{Pd–Al}) = 1.27$.
[81] H. Siebert, Anwendungen der Schwingungsspektroskopie in der anorganischen Chemie, Springer, Berlin, 1966.
[82] The decrease from $f(\text{PdC–O}) = 3.65$ mdyn $Å^{-1}$ to $f(\text{PdSi–O}) = 2.68$ mdyn $Å^{-1}$ is expected, since in relation a similar reduction is obtained between the force constants of e.g. $Cl_2C{=}O$ [83] and $Cl_2Si{=}O$ [84].
[83] H. Schnöckel, Z. Anorg. Allg. Chem. 460 (1980) 37.
[84] H. Schnöckel, J. Mol. Struct. 29 (1975) 129.